# Numerical Modeling of Delamination Resistance Improvement Through The Use of CNT-Reinforced Bonding Layers

Yassine El-Assami[1], Venkadesh Raman[2], Monssef DRISSI-HABTI[1,3,*]

1 - PRES LUNAM IFSTTAR, CS4 Route de Bouaye 44344 Bouguenais, France.
2 - Institut de Recherche Technologique (IRT) Jules VERNE, Chemin du Chaffault, 44340 Bouguenais, France.
3 - Director of the Consortium Durability of Intelligent Composite Materials (GIS DURSI)
*Corresponding Author (monssef.drissi-habti@ifsttar.fr)

**Keywords:** Composite materials, Carbon nanotubes, Homogenization, Finite elements

## ABSTRACT

The root-section is a high load carrying part of wind-turbine blade. The blade weight and stiffness properties are highly based on root-section material properties. Weight reduction is an essential factor for blade designers to improve the energy production. So, reducing the weight by keeping the structural stiffness is important for blade. Accordingly, we have proposed Carbon Nano-Tube (CNT) addition in composite material for the objective of increasing the structural reinforcement in root section. CNT alignment would help to improve interlaminar property. Adding CNT in polymers which is used in composite would increase the material stiffness; to balance that we can reduce the blade weight by decreasing section thickness or number of plies. Our numerical simulation concentrates to calculate the mechanical properties of CNT contained polymer RVE (Representative volume element) model. After identifying the dispersed CNT-polymer macroscopic properties, they are applied in a macro-scale model to prove their stiffness increment in-between composite plies.

## 1 INTRODUCTION

Carbon nanotubes (CNTs) are known for the best mechanical properties ever. Their Young's Modulus is around 5 times that of steel and their strength around 20 GPa [1]–[3]. These properties make them, theoretically, the best candidates to reinforce matrix like materials.

Despite their interesting properties, it is technically difficult to control their dispersion within a material. They tend to agglomerate if their concentration is high. That limits the amount of CNTs that can be added to a polymer matrix (maximum weight fraction of around 1% to 2% is usually reported in bibliography [4]–[7]). Even in small amounts, it is possible to achieve noticeable improvement of the mechanical properties of a polymer. At the scale of a structure, CNTs can be applied on some specific parts to improve the resistance of some high stressed regions.

In this work, polymer reinforcement with CNTs is studied at the atomic scale. We use a finite element (FEM) representative volume element (RVE) to calculate the improved properties of a CNT reinforced polymer.

It is known that CNTs are very slender and their length can reach few micrometres, while their diameter is of some nanometres. In reality, their shape is usually curved. Even though this model can handle long CNTs, for practical reasons, it will be used for CNTs short enough so that the effects of curvature can be neglected.

CNT atomic structure is modelled using molecular mechanics: an analogy between the C-C covalent bonds potential and the strain energy of Euler beam elements is considered. We choose to model the atomic structure of a CNT so that some geometrical parameters such as the chirality and some defects related to functionalization [8]–[10] can be controlled. As for polymers, it is more convenient to consider their engineering properties as their atomic structure is random. They are modelled as continuous media.

Interaction between a CNT and the surrounding atoms of a matrix is modelled using an interface that represents the average behaviour of van der Waals interactions. No covalent interaction is considered in this model.

In the following paper, the finite element model is briefly explained: CNT model, interface and RVE. Then, we evaluate the effect of reinforcement on the elastic properties of a nano-composite. An application is also proposed to show the benefit of CNTs onthe improvement of resistance to shear.

## 2 NUMERICAL MODEL

A FEM model is established to study the reinforcing effect of a CNT. The atomic structure of a CNT is simulated by a lattice of Euler beams which mechanical properties are related to the atomic potential of C-C covalent bonds. Polymers are modelled as classical continuous media and the interface as a continuous layer linking the CNT to the reinforced matrix.

### 2.1 Carbon nanotube structure

CNTs are allotropes of carbon of long cylindrical hollow structure. Their wall is formed by a graphene-like sheet, enrolled into a cylinder. Chirality is a geometrical that defines how the graphene sheet is enrolled. It controls the rolling direction,$\vec{C}$,and the diameter of the CNT. Chirality is defined with the pair $(n, m)$ as follows (figure 1):

$$\vec{C} = n\overrightarrow{a_1} + m\overrightarrow{a_2} \tag{1}$$

The structure of a CNT can be zigzag if $m = 0$, armchair if $m = n$ or chiral in the other cases.

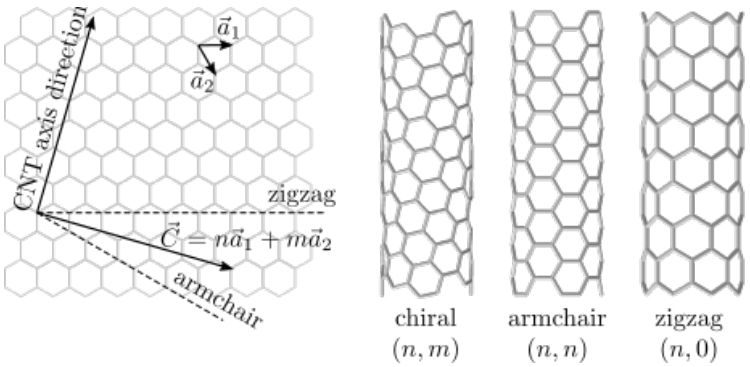


Figure 1: Rolling direction of a graphene sheet and types of chirality

The algorithm used in this work generates CNT structure based on the parameters $n, m$ and a given length, by enrolling a graphene sheet. As CNT diameters used in this work are small, the fact that CNTs are not capped does not influence the results.

### 2.2 CNT atomic model

To model a CNT in FEM, an analogy between C-C bonds and Euler beam elements is used. We consider, under the hypothesis of small deformation that the potential energy, $U_a$, for each couple of carbon atoms is equal to the elastic strain of a Euler beam, $U_b$.

$U_a$ is expressed as [9], [11]:

Stretching potential — Bending potential — Dihedral potential — Out-of-plane potential — Van der Waals potential — Electrostatic potential

$$\begin{aligned} U_a &= U_r + U_\theta + (U_\phi + U_\omega) + U_{vdW} + U_{es} \\ &= \frac{1}{2}k_r(\Delta L)^2 + \frac{1}{2}k_\theta(\Delta\theta)^2 + \frac{1}{2}k_\tau(\Delta\phi)^2 + \cancel{U_{vdW}} + \cancel{U_{es}} \end{aligned} \tag{2}$$

Stretching force constant — Bending force constant — Torsional constant — Negligible quantities

$k_r$, $k_\theta$ and $k_\phi$ are the bond force constants of stretching, bending and torsional resistance calculated from potential functions of molecular mechanics [11], [12]. $\Delta L$, $\Delta\theta$ and $\Delta\phi$ are the respectively the variations of bond length, bending and torsion angles.Van der Waals effect and electrostatic forces can be neglected in front of the terms relative to the bonded interaction.

$U_b$ is expressed as[9]:

Tension energy — Bending moment — Torsion energy

$$\begin{aligned} U_b &= U_A + U_M + U_T \\ &= \frac{1}{2}\frac{EA}{L}(\Delta L)^2 + \frac{1}{2}\frac{EI}{L}(\Delta\theta)^2 + \frac{1}{2}\frac{GJ}{L}(\Delta\phi)^2 \end{aligned} \quad (3)$$

$E$ and $G$ are the Young's and shear moduli of the beam. For a circular section, $A = \pi r^2$ is the section area, $I = \frac{\pi r^4}{4}$ its second moment and $J = \frac{\pi r^4}{2}$ its polar moment. Under the hypothesis of small strain, $E$, $G$ and $r$ are constants. Considering the equality between $U_a$ and $U_b$, we obtain:

$$r = 2\sqrt{\frac{k_\theta}{k_r}} \quad , \quad E = \frac{k_r^2 L}{4\pi k_\theta} \quad , \quad G = \frac{k_r^2 k_\tau L}{8\pi k_\theta^2} \quad (4)$$

$L = 0.1421$ nm is the equilibrium distance between two carbon atoms [12]. As for the bond constants, $k_r = 786$ nN/nm, $k_\theta = 0.901$ nN nm/rad$^2$ and $\nu = 0.0344$[13]. So, the Young's modulus of the beam elements is $E = 7753$ GPa and the section radius is $r = 0.0677$ nm.

### 2.2 Interface model

CNT is linked to the matrix by van der Waals forces, but covalent bonds can also be forced by CNT functionalization. Covalent bonds can be modelled with the same length, and each carbon atom has only one interaction with the matrix. Van der Waals interactions are however more difficult to model as they are neither of the same length nor the same behaviour.

In the present work, we consider that CNT is linked to the polymer only through van der Waals forces. The effective behaviour of the interface is modelled with a continuous layer that is different from the polymer. The thickness of this layer respects a distance of stability, $h$, between the CNT and polymer.

The interest of using a continuous layer is that it is simple to implement and its behaviour can be controlled taking into account engineering parameters rather that atomic data.

Jiang and al. [14] calculated a cohesive behaviour of the interface, based on the densities of interacting particles and atomic potential constants. This behaviour represents an average of the van der Waals interactions between a CNT and the reinforced polymer.

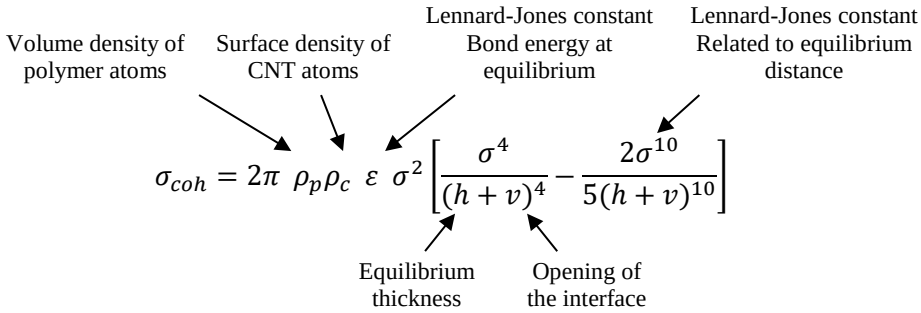


(5)

Equation (5) represents the stress $\sigma_{\mathrm{coh}}$ as a function of the opening v of a graphene sheet in interaction with a polymer matrix. It can be used for diameters higher than that of a $(\mathrm{n} = 5, \mathrm{m} = 5)$ CNT.The equilibrium distance between CNT and the polymer is $\mathrm{h} = \left(\frac{2}{5}\right)^{\frac{1}{6}}\sigma$.

Under the hypothesis of small strain, the cohesive low can be approximated by a linear behaviour of Young's modulus,$E_{\mathrm{int}}$, with a maximum stress equal to $\sigma_{\mathrm{coh}}^{\max}$ where:

$$E_{\mathrm{int}} = 30\left(\frac{2}{5}\right)^{\frac{1}{3}}\pi\rho_{\mathrm{p}}\rho_{\mathrm{c}}\varepsilon\sigma^2 \tag{6}$$

$$\sigma_{\mathrm{coh}}^{\max} = \sigma_{\mathrm{coh}}(\sigma - h) = \frac{6\pi}{5}\rho_p\rho_c\varepsilon\sigma^2 \tag{7}$$

For the following numerical simulations, $\sigma = 0.3825\ \mathrm{nm}$, $\varepsilon = 7.462 \times 10^{-4}\ \mathrm{nN \cdot nm}$ and $\rho_{\mathrm{c}} = \frac{4}{3\sqrt{3}L^2} = 38.1\ \mathrm{nm}^{-2}$[14]. As for $\rho_{\mathrm{p}}$, it can be estimated from the density of the polymer as the number of particles per volume unit $\rho_{\mathrm{p}} = 46.0\ \mathrm{nm}^{-3}$.

The cohesive law calculated for shear depends on the sliding displacement, the opening and the length of CNT. Jiang and al. [14] show that shear does not vanish even though there is no sliding displacement, but its value is much smaller than the cohesive tensile stress. To account for shear in the following simulations, a Poisson's ratio equal to that of the polymer is considered. Pull-out test results can for example also be used to calibrate sliding behaviour for more accuracy [15], [16].

## 3 INFLUENCE OF CNT ORIENTATION

Even though the mechanical properties of a CNT are very interesting, its high aspect ratio and the big difference between its stiffness and the stiffness of a polymer makes it difficult to predict the reinforced properties with classical mean field models. Morphological details are important to take into consideration. In what follows, an example is studied to show the influence of CNT orientation on the Young's modulus of a CNT reinforced polymer.

CNT is oriented in different directions and its orientation relative to the loading direction is controlled by an angle α.

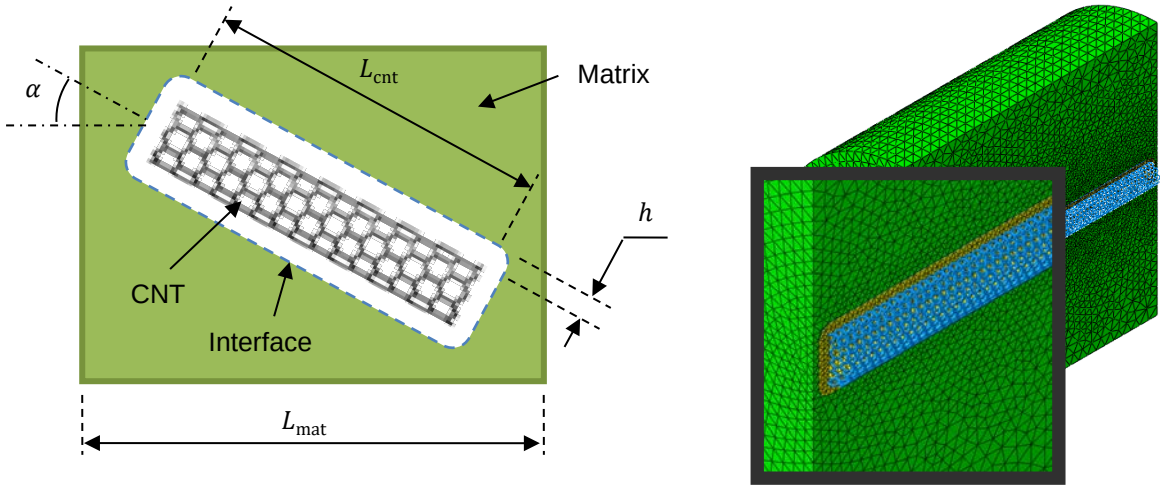


**Figure 2.**Description of the model and example of a used mesh.

The modelled CNT is armchair (10,10) (which corresponds to a diameter of 1.4 nm), with a length of 17 nm.The weight fraction is 1%. The RVE cylinder has a height of 18 nm and a diameter of 18 nm (schematic at figure 2). A short CNT has been chosen for this example so that its orientation can be varied in the range $[0°, 90°]$.

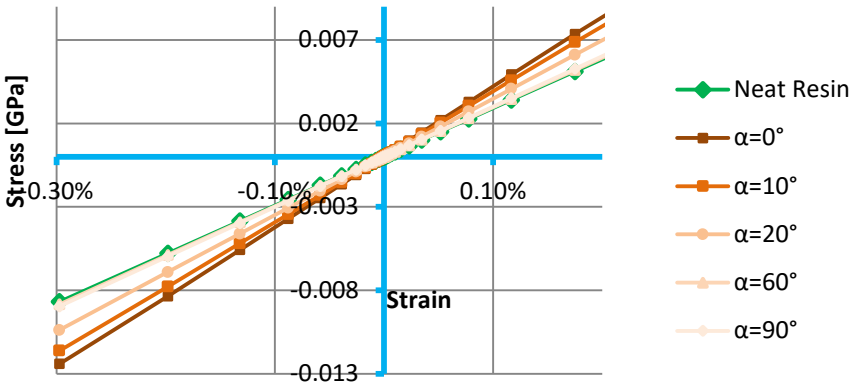


**Figure 3.** Strain-Stress curves relative to tension and compression simulations.

Figure 3 shows stress strain curves, relative to tension and compression simulations for different orientations α, compared to the curve of neat matrix. Stress is calculated from the reaction force, reported to the sectional area of the cylinder. Strain is equal to the displacement of the loaded end divided by the cylinder length.

As expected, stress is the highest when CNT is oriented in the load direction ($\alpha = 0°$). Stress-strain curves tend towards that of the neat resin as the orientation gets perpendicular.

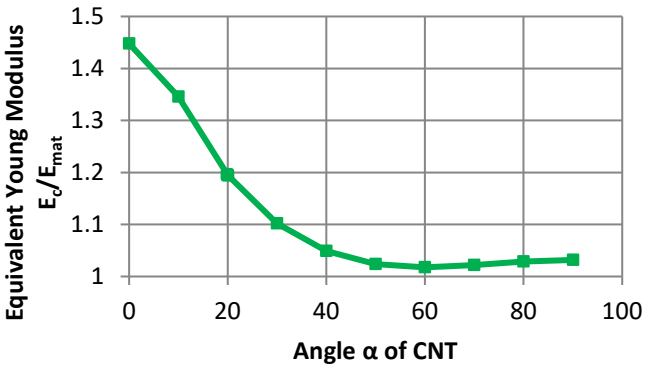


**Figure 4.** Young's modulus of the composite $E_c$ as a function of the CNT orientation α.

Figure 4 also shows the evolution of longitudinal Young's modulus of the composite, $E_c$, as a function of the angle α. At $\alpha = 0°$, the Young's modulus is the highest: an improvement of 45% is noticed (it does not however attain the value of modulus predicted by the law of mixture as the CNT is not infinitely long). When angle α is higher, CNT participates less to load transfer until the Young's modulus reaches a plateau value at $\alpha = 40°$, corresponding to an improvement of less than 5%.

## 4 HOMOGENIZATION OF ELASTIC BEHAVIOUR

The homogenization of the elastic properties of a given RVE consists in finding the relation between the macroscopic stress, $\langle\sigma\rangle$, and macroscopic strain $\langle\varepsilon\rangle$, where $\langle\cdot\rangle = \frac{1}{|\Omega|}\int_\Omega \cdot \, dV$ and Ω the domain of the RVE. However, numerical calculation of volume averages is not possible in this case, as CNT volume does not have a meaning in the present case.To encounter this problem, divergence theorem can be used to express volume averages as integrals on the outer border of the RVE $\partial\Omega$. An algorithm is established to calculate macroscopic fields from the boundary elements:

Macroscopic stress — Barycentre of the boundary facet $i$ — Surface traction $\mathbf{t}_i = \boldsymbol{\sigma}_i \cdot \mathbf{n}_i$ — Area of the boundary surface $i$

$$\langle\sigma\rangle \approx \frac{1}{|\Omega|}\sum_{i\in\partial\Omega^*} x_i \otimes t_i \, dS_i$$

$$\langle\varepsilon\rangle \approx \frac{1}{2|\Omega|}(\epsilon + \epsilon^T) \; where \; \epsilon = \sum_{i\in\partial\Omega^*} n_i \otimes u_i \, dS_i \tag{8}$$

Macroscopic strain — Volume of domain Ω — Boundary of domain Ω — Unit vector normal to facet $i$ — Displacement of facet $i$

Under the hypothesis of small strain, a linear relation can be considered between these two quantities, involving the macroscopic stiffness $\mathbb{C}_c$:

$$\langle\boldsymbol{\sigma}\rangle = \mathbb{C}_c : \langle\boldsymbol{\varepsilon}\rangle \tag{9}$$

At small strain, the response of the material is linear elastic. In order to calculate the effective stiffness tensor, $\mathbb{C}_c$, of equation (9), a FEM model of a cuboid RVE has been used (figure 6). A displacement u, compatible with a macroscopic strain $\langle\varepsilon\rangle$, is imposed on the border of the RVE: $u = \langle\varepsilon\rangle \cdot x$, where x is the coordinate of the points of the boundary. In order to obtain the whole

macroscopic stiffness tensor, compression simulations in 3 directions and shear simulations is 3 planes are needed (figure 5).

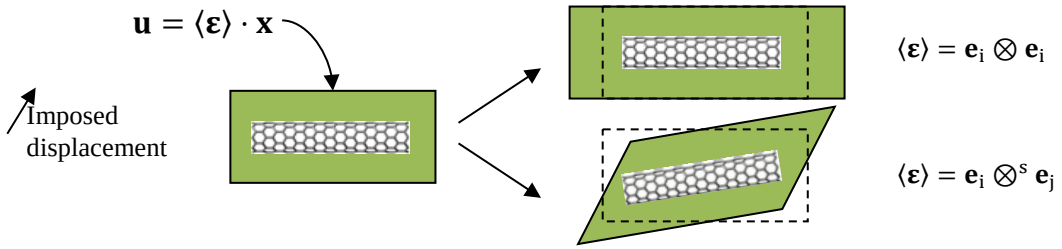


**Figure 5.** Schematic of boundary conditions needed to calculate the stiffness tensor.

In this model, CNT is completely embedded inside the matrix. A minimum distance equal to 2h is left from the border. In order to minimize the impact of the CNT length, an important aspect ratio has been considered so that the length of the CNT is close to the length of the RVE. The CNT is armchair (6,6) with a diameter of 0.82 nm and a length of 40 nm.

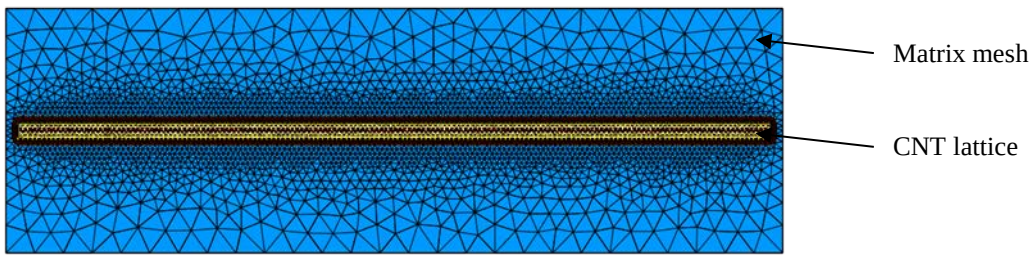


**Figure 6.** Longitudinal cut of RVE mesh.

As expected, the effective behaviour, calculated from the effective stiffness tensor $\mathbb{C}_c$ with equation (8), is transversely isotropic, as shows table 1:

| | $E_1$ (GPa) | $E_3$ (GPa) | $\nu_{12}$ | $\nu_{13}$ | $G_{13}$ (GPa) | $G_{12}$ (GPa) |
|---|---|---|---|---|---|---|
| Neat Polymer Matrix | 2.92 | 2.92 | 0.4 | 0.4 | 1.04 | 1.04 |
| Nanocomposite | 3.21 | 5.67 | 0.5 | 0.2 | 1.06 | 1.06 |
| Ratio | 1.10 | 1.94 | - | - | 1.01 | 1.01 |

**Table 1.**Homogenized properties and comparison with neat polymer matrix.

The Young's modulus is doubled in the direction of the CNT with only 1% of weight fraction. The transverse Young's modulus is improved by 10%. The improvement of the elastic shear moduli is however very low.

## 5 RESISTANCE TO SHEAR

CNTs can be used to improve some parts of the structure that are most likely to be vulnerable to some kind of loading. In what follows, an application is proposed to point-out the improvement of resistance to delamination. CNT reinforced joints can be applied between the plies to increase shear strength (figure 7).

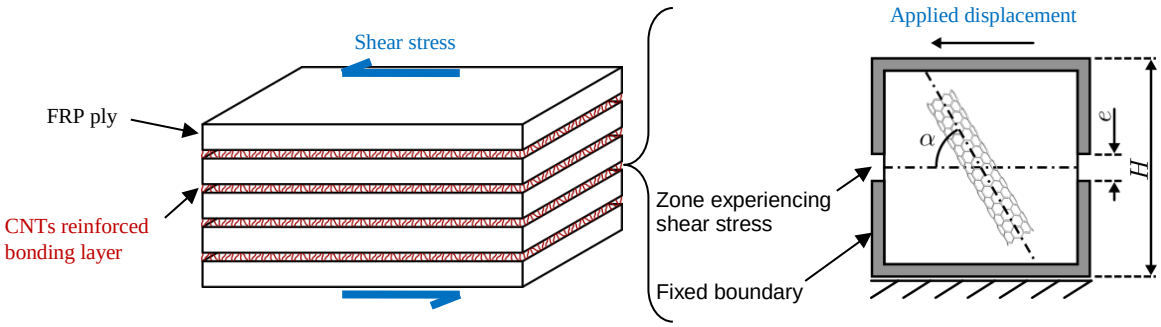


**Figure 7.** Schematic of bonding layer reinforced with a CNT, experiencing shear stress.

In order to evaluate the effect of CNTs in a bonding layer, we consider a cuboidal domain of polymer containing a CNT, loaded under shear. Three areas are virtually defined in this cuboid, based on the boundary conditions: an upper and a lower areas of the same size, separated by a thin area experiencing shear (figure 7). The upper and lower areas are considered as if they were inside infinitely rigid nano-grips. The boundary of the lower area is fixed and a displacement is applied on the boundary of the upper area, subjecting the middle region to shear stress.

An elastoplastic model is used to account for the nonlinear behavior of the matrix. CNT orientation is controlled by angle α ($\alpha = 0°$: the CNT is parallel to shear plane. $\alpha = 90°$: the CNT is perpendicular to shear plane).

We follow the evolution of the resultant force applied of the upper boundary as a function of the its displacement (figure 8). The resultant force is normalized by the maximum force obtained in a simulation without CNT and the displacement is normalized by the thickness of the area under shear.

As known, the neat polymer resin breaks in a brittle way once the shear strength is reached. In this case, the entire middle region reaches its maximum stress and the neat matrix separates in two independent blocks. In the case of the RVE representing the bond joint reinforced by the CNT, once shear stress is applied, the effect of nano-reinforcement can be observed. Hence, the RVE will deform in a non-linear way. The simulations are plotted in figure 8, where a comparison is made between the cases of the neat resin versus the nano-reinforced resin with the CNT that was oriented at various directions α.

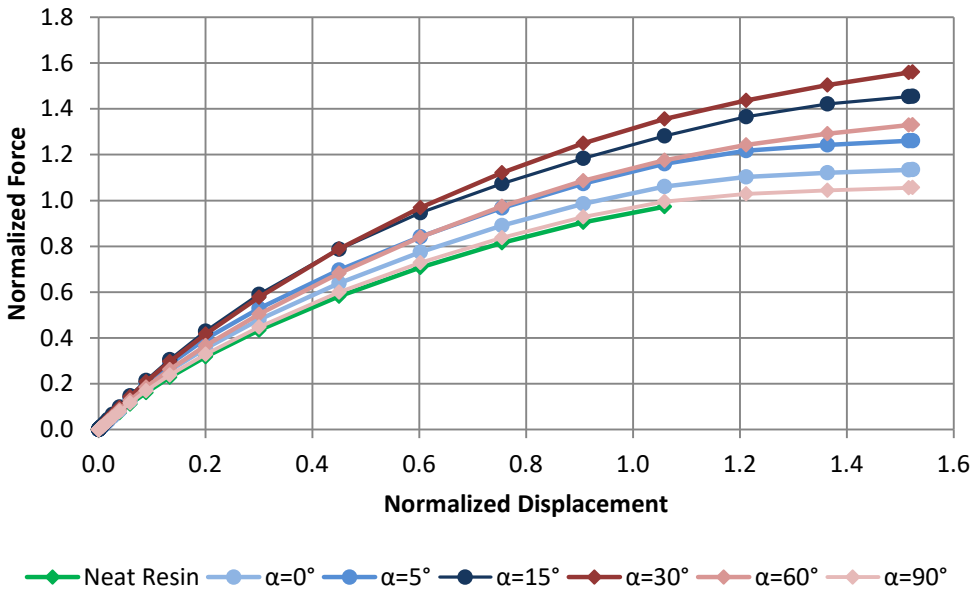

**Figure 8.** Resultant force applied on the upper boundary as a function of the boundary displacement. The resultant is normalized by maximum force of the unreinforced polymer and displacement is normalized by the middle layer thickness.

The CNT strengthens the matrix by transferring a part of the applied load from upper to lower regions. It can be noticed that the strengthening effect is higher when the CNT orientation, α, is in the range 15° to 45°; resistance to shear is provided through the C–C covalent bonds. For angles lower than 15°, it seems that shear is mostly resisted by the CNT-polymer interface, which explains the drop in resistance. For higher orientation angles, another drop in the resistance is noticed. This can be explained by the fact that the CNT is more efficient while under tension than under pure shear. An increase in the shear resistance up to 40% is observed.

## 6 CONCLUSION

In order to produce high performance polymers, CNTs are very promising to attain improved mechanical properties. This improvement is stands however limited because of the difficulty to achieve a good impregnation and dispersion of CNTs when the weight fraction is high.

The high aspect ratio of CNTs, their low weight fraction and their high stiffness makes it difficult to use classical methods to homogenize the mechanical behaviour. Detailed models are needed to take into account the high anisotropy. Indeed, the model used here shows a big influence of some morphological details such as CNT orientation.

As the control of CNTs orientation is technically difficult to achieve industrially, the mechanical behaviour is not optimal in the reality. But the loss of elastic stiffness due to the random dispersion of CNTs is out-balanced by the improvement of other resistance mechanisms, such as shear strength, as emphasized in the last simulations.

One of the advantages of the model that was developed is that it is suitable to handle CNTs of sizes that are industrially available (lengths in the range 40 - 100 nm were used in current simulations). It is also possible to consider local defects on the CNT atomic lattice, due to functionalization for example, as well as stronger bonds on the interface.

## 7 REFERENCES

[1] R. S. Ruoff, D. Qian, and W. K. Liu, 'Mechanical properties of carbon nanotubes: theoretical predictions and experimental measurements', *Comptes Rendus Phys.*, vol. 4, no. 9, pp. 993–1008, Nov. 2003.

[2] M. Meo and M. Rossi, 'Prediction of Young's modulus of single wall carbon nanotubes by molecular-mechanics based finite element modelling', *Compos. Sci. Technol.*, vol. 66, no. 11–12, pp. 1597–1605, Sep. 2006.

[3] K. I. Tserpes, P. Papanikos, and S. A. Tsirkas, 'A progressive fracture model for carbon nanotubes', *Compos. Part B Eng.*, vol. 37, no. 7–8, pp. 662–669, Oct. 2006.

[4] D. Qian, E. C. Dickey, R. Andrews, and T. Rantell, 'Load transfer and deformation mechanisms in carbon nanotube-polystyrene composites', *Appl. Phys. Lett.*, vol. 76, no. 20, pp. 2868–2870, May 2000.

[5] B. Fiedler, F. H. Gojny, M. H. G. Wichmann, M. C. M. Nolte, and K. Schulte, 'Fundamental aspects of nano-reinforced composites', *Compos. Sci. Technol.*, vol. 66, no. 16, pp. 3115–3125, Dec. 2006.

[6] A. Montazeri and N. Montazeri, 'Viscoelastic and mechanical properties of multi walled carbon nanotube/epoxy composites with different nanotube content', *Mater. Des.*, vol. 32, no. 4, pp. 2301–2307, Apr. 2011.

[7] F. Vahedi, H. R. Shahverdi, M. M. Shokrieh, and M. Esmkhani, 'Effects of carbon nanotube content on the mechanical and electrical properties of epoxy-based composites', *New Carbon Mater.*, vol. 29, no. 6, pp. 419–425, Dec. 2014.

[8] G. M. Odegard, T. S. Gates, L. M. Nicholson, and K. E. Wise, 'Equivalent-continuum modeling of nano-structured materials', *Compos. Sci. Technol.*, vol. 62, no. 14, pp. 1869–1880, Nov. 2002.

[9] C. Li and T.-W. Chou, 'A structural mechanics approach for the analysis of carbon nanotubes', *Int. J. Solids Struct.*, vol. 40, no. 10, pp. 2487–2499, May 2003.

[10] C. Li and T.-W. Chou, 'Multiscale Modeling of Carbon Nanotube Reinforced Polymer Composites', *J. Nanosci. Nanotechnol.*, vol. 3, no. 5, pp. 423–30, 2003.

[11] A. K. Rappe, C. J. Casewit, K. S. Colwell, W. A. Goddard, and W. M. Skiff, 'UFF, a full periodic table force field for molecular mechanics and molecular dynamics simulations', *J. Am. Chem. Soc.*, vol. 114, no. 25, pp. 10024–10035, Dec. 1992.

[12] D. W. Brenner, O. A. Shenderova, J. A. Harrison, S. J. Stuart, B. Ni, and S. B. Sinnott, 'A second-generation reactive empirical bond order (REBO) potential energy expression for hydrocarbons', *J. Phys. Condens. Matter*, vol. 14, no. 4, p. 783, 2002.

[13] X. Lu and Z. Hu, 'Mechanical property evaluation of single-walled carbon nanotubes by finite element modeling', *Compos. Part B Eng.*, vol. 43, no. 4, pp. 1902–1913, Jun. 2012.

[14] L. Y. Jiang *et al.*, 'A cohesive law for carbon nanotube/polymer interfaces based on the van der Waals force', *J. Mech. Phys. Solids*, vol. 54, no. 11, pp. 2436–2452, Nov. 2006.

[15] S. Namilae and N. Chandra, 'Multiscale Model to Study the Effect of Interfaces in Carbon Nanotube-Based Composites', *J. Eng. Mater. Technol.*, vol. 127, no. 2, pp. 222–232, Apr. 2005.

[16] Y. L. Chen, B. Liu, X. Q. He, Y. Huang, and K. C. Hwang, 'Failure analysis and the optimal toughness design of carbon nanotube-reinforced composites', *Compos. Sci. Technol.*, vol. 70, no. 9, pp. 1360–1367, Sep. 2010.